

Production of K^{*0} in Au+Au collisions at $\sqrt{s_{NN}} = 19.6$ GeV from RHIC BES-II

Aswini Kumar Sahoo (for the STAR collaboration)^{1,*}

¹Indian Institute of Science Education and Research, Berhampur, 760010, India

Abstract. We present the study of K^{*0} in Au+Au collisions at $\sqrt{s_{NN}} = 19.6$ GeV from RHIC BES-II. The ratio of resonance to non-resonance (K^{*0}/K) is shown as function of centrality and center-of-mass energy, which implies the dominance of hadronic re-scattering over regeneration in central A+A collisions. The lower limit of hadronic phase lifetime ($t_{kin} - t_{chem}$) is also reported using a toy model ansatz. The results are compared with previous RHIC and LHC measurements.

1 Introduction

Relativistic heavy-ion collisions provide a unique opportunity to understand the deconfined state of matter called the Quark-Gluon Plasma. The short-lived hadronic resonances are a very good probe to study the hadron gas phase, which characterises the late-stage evolution of heavy-ion collisions. $K^{*0}(892)$ has a lifetime ~ 4.16 fm/c which is smaller compared to that of fireball (~ 10 fm/c). Due to its short lifetime, the decay daughters may interact with the medium and change the properties of the resonances. In between chemical (CFO) and kinetic (KFO) freeze out, the daughter particles of $K^{*0}(892)$ could undergo in-medium effects like re-scattering and regeneration. Hence the final yield of the $K^{*0}(892)$ depends on the interplay of these effects, and can be used to study the hadronic phase of heavy-ion collisions [1].

2 Data Sets and Analysis Details

In these proceedings, we report the production yield of K^{*0} meson in Au+Au collisions at $\sqrt{s_{NN}} = 19.6$ GeV, accumulated by the STAR experiment in 2019 as part of the RHIC BES-II program. The $K^{*0}(\overline{K^{*0}})$ is reconstructed via its decay channel $K^{*0}(\overline{K^{*0}}) \rightarrow K^+\pi^- (K^-\pi^+)$. The vertex positions along the beam (V_z) and radial (V_r) directions are required to be within $|V_z| < 145$ cm and $|V_r| < 2$ cm. The daughter particles are identified using both the Time Projection Chamber (TPC) and the Time Of Flight (TOF) detector. In BES-II, the inner part of the TPC has been upgraded for better momentum resolution, wider transverse momentum (p_T) and pseudo-rapidity coverages.

The combinatorial background is estimated using the track rotation method, where one of the daughter (here π) track momentum is rotated by 180° in transverse plane in order to break the correlation among the pairs originating from same parent resonance (K^{*0}). The K^{*0} signal is obtained after subtracting the combinatorial background from the same event $K\pi$ pairs,

*e-mail: aswinikumar.aks96@gmail.com

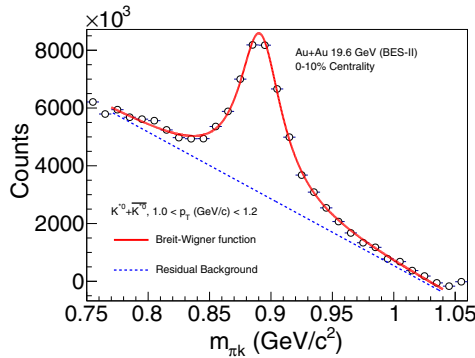


Figure 1. K^{*0} signal for $1.0 < p_T < 1.2$ GeV/c in 0-10% Au+Au collisions at $\sqrt{s_{NN}} = 19.6$ GeV.

which is then fitted with the Breit-Wigner function and a first-order polynomial representing the residual background. Figure 1 shows an example of K^{*0} signal extraction for $1.0 < p_T < 1.2$ GeV/c in 0-10% Au+Au collisions at $\sqrt{s_{NN}} = 19.6$ GeV. The yield is estimated by integrating the signal within $0.77 < m_{\pi K} < 1.04$ GeV/c² after residual background subtraction.

3 Results

3.1 Particle ratios

If the K^{*0} meson decays before KFO, the decay daughters (π and K) can re-scatter with other hadrons present in the medium, so that their momenta may get changed. Hence, one may not be able to reconstruct the parent resonance. On the other hand pions and kaons present in the medium may regenerate K^{*0} via pseudo-elastic scattering ($\pi K \rightarrow K^{*0}$). Hence the yield of the resonance is controlled by the relative contribution of these in-medium effects. The resonance to non resonance ratio (K^{*0}/K) can help us probe this phenomenon.

The left panel of Fig. 2 shows the K^{*0}/K and ϕ/K ratio as a function of the average number of participating nucleons $\langle N_{part} \rangle$. Here, we observe that the K^{*0}/K ratio decreases from peripheral to central collisions, while ϕ/K remains almost constant throughout all centralities. The thermal model prediction overestimates the K^{*0}/K , whereas the ϕ/K ratio is consistent with the prediction. In right panel of Fig. 2 we present K^{*0}/K as a function of collision energy for both elementary and heavy-ion collisions. Here we observe the ratio in A+A collisions is suppressed as compared to the elementary collisions. All these measurements indicate a dominant hadronic re-scattering effect over regeneration in central A+A collisions. The ϕ meson, which has a long lifetime (~ 46 fm/c), may remain immune to these in-medium effects.

3.2 Hadronic phase lifetime

Here the time difference between CFO and KFO is considered as the hadronic phase lifetime. Since it's span can not be measured directly, we can use the K^{*0}/K ratio to extract the lower limit of hadronic phase lifetime [1] using the following [24] relation:

$$\left(\frac{K^{*0}}{K}\right)_{KFO} = \left(\frac{K^{*0}}{K}\right)_{CFO} \times e^{-\Delta t/\tau_{K^{*0}}}, \quad (1)$$

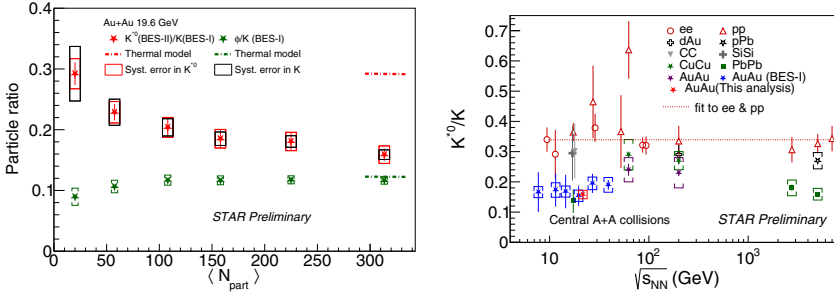


Figure 2. Left panel: Resonance to non-resonance ratio as a function of $\langle N_{part} \rangle$ along with the thermal model prediction. Here K^{*0}/K and ϕ/K (BES-I)[2] denotes $(K^{*0} + \bar{K}^{*0})/(K^+ + K^-)$ and $2\phi/(K^+ + K^-)$ respectively. Here the K^{*0} measurement is based on BES-II data, whereas the measurement of kaons is from BES-I [3]. Hence their systematic uncertainties are denoted by different boxes. Right panel: K^{*0}/K as a function of collision energy [4–23]. The bars and caps (boxes) denote the statistical and systematic uncertainties respectively.

Here the $(K^{*0}/K)_{CFO}$ and $(K^{*0}/K)_{KFO}$ are taken to be the K^{*0}/K ratios measured in elementary and heavy-ion collisions respectively. This method assumes that no K^{*0} regeneration takes place between the chemical and kinetic freeze out, and all K^{*0} that decay before the kinetic freeze out are lost due to the re-scattering effect. The calculated Δt is boosted by the lorentz factor which is estimated as $\sqrt{1 + (\langle p_T \rangle / mc)^2}$.

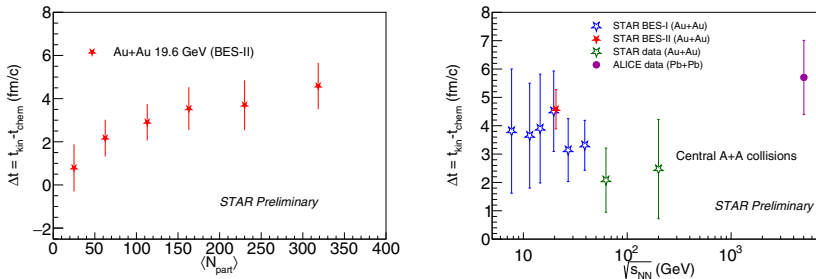


Figure 3. Left panel: Lower limit of hadronic phase lifetime (Δt) as a function of $\langle N_{part} \rangle$. Right panel: Lower limit of hadronic phase lifetime (Δt) as a function of collision energy. The result is compared with previous STAR and ALICE measurements [11, 13, 25]. The error bars are the quadratic sum of statistical and systematic uncertainties.

The left panel of Fig. 3 denotes the lower limit of hadronic phase lifetime as a function of N_{part} . The lifetime seems to increase from central to peripheral collisions. In the right panel of Fig. 3, Δt is plotted as a function of $\sqrt{s_{NN}}$ for central A+A collisions. RHIC measurement seems to be smaller compared to that of LHC, but the measurement uncertainties are large.

4 Summary

Measurement of K^{*0} at mid-rapidity in Au+Au collisions at 19.6 GeV (BES-II) is presented. The K^{*0}/K in central collisions appears to be less than that in peripheral collisions, and also the ratio is suppressed in heavy-ion collisions in comparison with elementary collisions. On the other hand, ϕ/K remains almost independent of centrality. This suggests that the hadronic phase formed in A+A collisions is mostly re-scattering dominated. The lower limit of hadronic phase lifetime is estimated using the K^{*0}/K ratio, which seems to be smaller as compared to LHC measurements in central heavy-ion collisions. A study with high statistics BES-II data across various energies is needed to draw definitive conclusions.

References

- [1] C. Adler et al. (STAR), Phys. Rev. C **66**, 061901 (2002)
- [2] J. Adam et al. (STAR), Phys. Rev. C **102**, 034909 (2020)
- [3] L. Adamczyk et al. (STAR), Phys. Rev. C **96** (2017)
- [4] H. Albrecht et al. (ARGUS), Z. Phys. C **61**, 1 (1994)
- [5] Y.J. Pei, Z. Phys. C **72**, 39 (1996)
- [6] W. Hofmann, Ann. Rev. Nucl. Part. Sci. **38**, 279 (1988)
- [7] K. Abe et al. (SLD), Phys. Rev. D **59**, 052001 (1999)
- [8] M. Aguilar-Benitez et al., Z. Phys. C **50**, 405 (1991)
- [9] T. Akesson et al. (Axial Field Spectrometer), Nucl. Phys. B **203**, 27 (1982)
- [10] A. Adare et al. (PHENIX), Phys. Rev. C **90**, 054905 (2014)
- [11] J. Adams et al. (STAR), Phys. Rev. C **71**, 064902 (2005)
- [12] B.I. Abelev et al. (STAR), Phys. Rev. C **78**, 044906 (2008)
- [13] M.M. Aggarwal et al. (STAR), Phys. Rev. C **84**, 034909 (2011)
- [14] T. Anticic et al. (NA49), Phys. Rev. C **84**, 064909 (2011)
- [15] A. Aduszkiewicz et al. (NA61/SHINE), Eur. Phys. J. C **80**, 460 (2020)
- [16] B.B. Abelev et al. (ALICE), Phys. Rev. C **91**, 024609 (2015)
- [17] J. Adam et al. (ALICE), Phys. Rev. C **95**, 064606 (2017)
- [18] S. Acharya et al. (ALICE), Phys. Lett. B **802**, 135225 (2020)
- [19] B. Abelev et al. (ALICE), Eur. Phys. J. C **72**, 2183 (2012)
- [20] S. Acharya et al. (ALICE), Phys. Rev. C **102**, 024912 (2020)
- [21] S. Acharya et al. (ALICE), Phys. Lett. B **807**, 135501 (2020)
- [22] S. Acharya et al. (ALICE) (2021), 2110.10042
- [23] J. Adam et al. (ALICE), Eur. Phys. J. C **76**, 245 (2016)
- [24] S. Singha et al., Int. J. Mod. Phys. E **24**, 1550041 (2015)
- [25] S. Acharya et al. (ALICE), Phys. Lett B **802**, 135225 (2020)